http://www.kidney-international.org

Activation of innate immune defense mechanisms contributes to polyomavirus BK-associated nephropathy

Andrea Ribeiro[1,8], Markus Wörnle[1,8], Nasim Motamedi[2], Hans J. Anders[1], Elisabeth F. Gröne[3], Hans Nitschko[2], Peter Kurktschiev[1], Hanna Debiec[4], Matthias Kretzler[5], Clemens D. Cohen[1,3], Hermann J. Gröne[6], Detlef Schlöndorff[1,7] and Holger Schmid[1]

[1]Medizinische Poliklinik Campus Innenstadt, Klinikum der LMU, Munich, Germany; [2]Department of Virology, Max von Pettenkofer-Institute, Munich, Germany; [3]Divison of Nephrology and Institute of Physiology, University of Zurich, Zurich, Switzerland; [4]INSERM UMR S 702, Paris, France; [5]Department of Medicine, University of Michigan, Ann Arbor, Michigan, USA; [6]Department of Cellular and Molecular Pathology, German Cancer Research Center, Heidelberg, Germany and [7]Department of Medicine, Mount Sinai School of Medicine, New York, New York, USA

Polyomavirus-associated nephropathy (PVAN) is a significant complication after kidney transplantation, often leading to premature graft loss. In order to identify antiviral responses of the renal tubular epithelium, we studied activation of the viral DNA and the double-stranded RNA (dsRNA) sensors Toll-like receptor 3 (TLR3) and retinoic acid inducible gene-I (RIG-I) in allograft biopsy samples of patients with PVAN, and in human collecting duct cells in culture after stimulation by the dsRNA mimic polyriboinosinic:polyribocytidylic acid (poly(I:C)), cytokines, or infection with BK virus. Double staining using immunofluorescence for BK virus and TLR3 showed strong signals in epithelial cells of distal cortical tubules and the collecting duct. In biopsies microdissected to isolate tubulointerstitial lesions, TLR3 but not RIG-I mRNA expression was found to be increased in PVAN. Collecting duct cells in culture expressed TLR3 intracellularly, and activation of TLR3 and RIG-I by poly(I:C) enhanced expression of cytokine, chemokine, and IFN-β mRNA. This inflammatory response could be specifically blocked by siRNA to TLR3. Finally, infection of the collecting duct cells with BK virus enhanced the expression of cytokines and chemokines. This led to an efficient antiviral immune response with TLR3 and RIG-I upregulation without activation of IL-1β or components of the inflammasome pathway. Thus, PVAN activation of innate immune defense mechanisms through TLR3 is involved in the antiviral and anti-inflammatory response leading to the expression of proinflammatory cytokines and chemokines.

Kidney International (2012) **81,** 100–111; doi:10.1038/ki.2011.311; published online 14 September 2011

KEYWORDS: immunology and pathology; renal tubular epithelial cells; transplantation

Correspondence: *Holger Schmid, Medizinische Poliklinik Campus Innenstadt, Klinikum der LMU, Pettenkoferstrasse 8a, D-80336 München, Germany. E-mail: holger.schmid@lrz.uni-muenchen.de*

[8]These authors contributed equally to this work.

Received 7 January 2011; revised 6 June 2011; accepted 12 July 2011; published online 14 September 2011

Polyomavirus-associated nephropathy (PVAN) is an emerging cause of significant kidney transplant dysfunction affecting up to 10% of organ recipients, often leading to graft loss. Most cases of PVAN are elicited by BK virus (BKV) in the context of intense immunosuppression. As no specific antiviral drug is available to date, the primary treatment for PVAN is reduction of immunosuppression, which must be carefully balanced against increased risks of acute rejection (AR).[1,2]

BKV normally replicates in urothelial cells, which remains asymptomatic in two-thirds of infected patients after kidney transplantation,[3] but it can exhibit tropism for the renal tubular epithelium, which may be latently infected.[4]

The renal involvement in PVAN is multifocal, and distal nephron segments, that is, medullary collecting ducts and distal cortical tubules, are usually more severely affected than proximal segments.[5] To achieve a productive infection, the BKV genome has to be delivered to the nucleus, where early genes are expressed, followed by DNA replication, late protein expression, and virion assembly. Histologically, viral replication results in tubular epithelial cell enlargement, karyomegaly, and nuclear inclusion bodies. These cytopathic changes are often associated with death of tubular epithelial cells, denudation of the basement membrane, and a strong interstitial inflammatory response, similar to that seen in acute interstitial rejection. Histological diagnosis of PVAN requires evaluation of a renal biopsy with demonstration of cytopathic changes and confirmation by immunohistochemistry.[6]

The molecular events involved in BKV invasion of host cells and subsequent intracellular trafficking are an important area of study. In various cell culture models, BKV uses an N-linked glycoprotein containing an α(2,3)-linked sialic acid as a receptor and enters cells through caveola-mediated endocytosis.[7,8] After this relatively slow and cholesterol-dependent internalization, BKV migrates through the cytoplasm and via cellular components to the nucleus, where viral transcription, replication, and assembly take place. The

innate immune system has a critical role in recognizing viral infections and evoking initial antiviral responses. Viruses are sensed via their nucleic acid genome or as a result of their replicative or transcriptional activity.[9] Several classes of receptors sense cytosolic viral components, such as double-stranded RNA (dsRNA), single-stranded RNA (ssRNA), and ds or ss DNA. These include retinoic acid-inducible gene I (RIG-I)-like receptors, Toll-like receptors (TLRs), nucleotide oligomerization domain-like receptors, and cytosolic DNA sensors.[10,11] Recognition by these sensors induces the production of type I interferons (IFNs) and the assembly of inflammasome complexes that activate caspase-1, leading to production of interleukin-1β (IL-1β) and IL-18.[12,13]

For polyomavirus BK, dsDNA and dsRNA are critical targets. The dsRNA is a molecular pattern associated with viral infection, because it is produced by most viruses at some point during their replication.[14] The recognition of viral dsRNA triggers downstream signaling cascades leading to the activation of nuclear factor (NF)-κB, and induces antiviral mediators such as type I IFNs and proinflammatory cytokines.[15,16] RIG-I is a highly inducible cytoplasmic RNA helicase that signals antiviral responses after binding dsRNA and ssRNA containing a 5′ triphosphate. This pathway has been implicated in antiviral responses to Sendai virus, vesicular stomatitis virus, Newcastle disease virus, as well as different flaviviruses and Kaposi's sarcoma-associated herpesvirus.[17–19] In addition, Chiu *et al.*[20] recently demonstrated that a cytosolic B form of dsDNA, poly (dA-dT) · poly (dA-dT), is able to activate RIG-I and induce IFN-β production via the cytosolic DNA-dependent RNA polymerase III (PolIII).

Because of the above-mentioned characteristics involved in BKV invasion of host cells and subsequent intracellular trafficking, we restricted our search for TLR candidates that could be involved in PVAN to those intracellular TLRs that sense nucleic acids in endosomal compartments. This latter group includes TLR3, TLR7, TLR8, and TLR9. Whereas TLR7 and TLR8 recognize ssRNA and TLR9 specifically binds CpG DNA motifs and has a significant role in the development of tubulointerstitial injury in systemic lupus,[21] TLR3 recognizes viral dsRNA, which is generated during the life cycle of many viruses, and its synthetic analog polyriboinosinic:polyribocytidylic acid (poly(I:C)).[22,23] TLR3 senses dsRNA through its unique adaptor protein TIR-domain-containing adapter-inducing interferon-β (TRIF).[24] Recognition of viral RNA by TLR3 triggers activation of the transcription factors NF-κB and interferon regulatory factor 3 and induction of type I IFNs, which are critical for cellular antiviral responses.

We hypothesized that particularly TLR3 could be a receptor candidate to mediate activation of innate immunity in PVAN. Our hypothesis was underscored by two recent findings. (1) TLR3 resides in the endosomal membrane and the endoplasmic reticulum and moves to dsRNA-containing endosomes in response to dsRNA.[25] As BKV has previously been shown to enter cells through endocytosis, viral dsRNAs could activate TLR3 during BKV infection of tubular epithelial cells upon viral entry and uncoating in the endosome. (2) Upregulation of the TLR3 pathway was reported in response to various viruses containing a dsDNA genome, for example, Kaposi's sarcoma-associated herpesvirus,[26] HSV-1,[27,28] and murine CMV.[29]

Here we examined the activation of TLR3 and RIG-I in allograft biopsy samples of PVAN and in human collecting duct cells after poly(I:C) and cytokine stimulation, as well as after infection with BKV. Our findings indicate that activation of innate immune defense mechanisms, that is, TLR3, contributes to the inflammation in PVAN.

RESULTS

In biopsies with PVAN staining for polyomavirus (anti-SV40) and TLR3 colocalized in epithelial cells of cortical tubules and the collecting duct

Polyomavirus BK exhibits a tropism for the renal tubular epithelium, particularly in distal nephron segments. Immunofluorescence double staining (Figure 1) for the SV40 large T antigen (T-Ag) of polyomavirus and TLR3 in allograft biopsies with histological diagnosis of PVAN showed

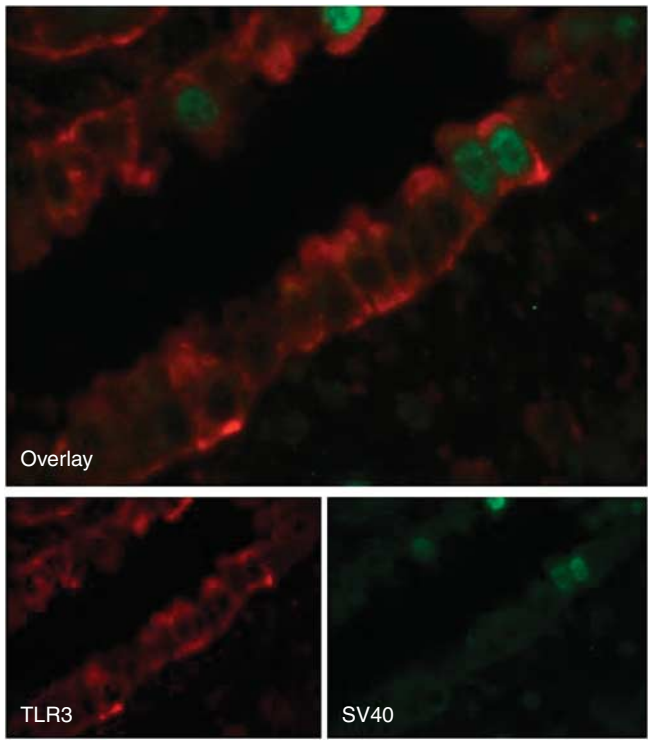

Figure 1 | Immunofluorescence double staining for Toll-like receptor 3 (TLR3) and SV40 in human kidney biopsies with clinical and histological diagnosis of polyomavirus-associated nephropathy (PVAN): colocalization of polyomavirus (anti-SV40) and TLR3 protein expression in epithelial cells of distal cortical tubules and the collecting duct. Double immunofluorescence staining of paraffin-embedded tissue sections of kidney needle biopsies from individuals with PVAN. Colocalization of nuclear signals for polyomavirus (SV40, green) and intracytoplasmatic signals for TLR3 (red) in tubular epithelial cells of distal cortical tubules and the collecting duct.

colocalization of nuclear signals for polyomavirus and intracytoplasmatic signals for TLR3 in epithelial cells of distal cortical tubules and the collecting duct. Intensity of immunofluorescence signals and SV40/TLR3 colocalization was semiquantitatively and separately assessed in medullary collecting ducts and cortical tubules. The results are summarized in Table 1. In general, we found a great variation in SV40 and TLR3 signal intensity in the different biopsies, with an overall most intense TLR3 staining in medullary collecting ducts of PVAN. Highest semiquantitative SV40/TLR3 colocalization rates (partially $>75\%$) were found in collecting ducts of the medulla in biopsies with few interstitial infiltrates. TLR staining in renal transplant biopsies without BKV infection was significantly less intense than in PVAN, and revealed a more cortical accentuated pattern with a most prominent TLR3 expression in cortical atrophic and dilated tubules.

TLR3 mRNA expression, but not RIG-I mRNA expression, is significantly induced in biopsies with PVAN compared with allograft biopsies with ongoing AR

We found a significant induction of TLR3 mRNA expression in the tubulointerstitial compartment of PVAN compared with renal allograft biopsies with AR and pretransplant donor biopsies. Despite similar inflammatory infiltrates by immunohistochemical analysis (see Supplementary Table S1 online), the increased expression of TLR3 mRNA in PVAN clearly differentiated them from those with AR (Figure 2a). In contrast, in renal allograft biopsies with AR, RIG-I mRNA expression was significantly induced compared with PVAN and controls (Figure 2b). As expected, according to the equally intense inflammatory infiltrate, the mRNA expression of CCL5 (chemokine (C-C motif) ligand 5)/RANTES (regulated upon activation, normal T cell expressed and secreted) was significantly upregulated in both AR and PVAN when compared with controls (Figure 2c).

Expression of TLR3 and RIG-I protein and mRNA on HCDCs in culture is enhanced after stimulation with poly(I:C) and proinflammatory cytokines

To confirm the expression of TLR3 protein on human collecting duct epithelial cells (HCDCs), fluorescence-activated cell sorting (FACS) analysis was conducted with a TLR3-specific monoclonal antibody as reported.[30] No detectable surface staining for TLR3 was found on HCDCs under basal conditions. As TLR3 has been described as an intracellular, vacuolar receptor, HCDCs were permeabilized before TLR3 staining and FACS analysis. This resulted in a robust TLR3 staining of HCDCs (Figure 3a).

To test whether HCDCs might express other TLRs, we screened for mRNA of TLR1–TLR10 by real-time reverse transcriptase-PCR (RT-PCR) under basal conditions. In addition to TLR3, HCDCs also robustly expressed TLR1, TLR2, TLR4, TLR5, TLR6, and TLR9. The expression for TLR7 and TLR10 was too low to allow evaluation, and no expression was found for TLR8 (data not shown).

To confirm TLR3 expression and to test the expression of RIG-I protein on HCDCs, western blot analysis was conducted with specific monoclonal antibodies for TLR3 and RIG-I (Figure 3b). Nonstimulated HCDCs revealed slight TLR3 and moderate RIG-I basal protein expression. After stimulation by poly(I:C) (10 μg/ml) as a mimetic of viral dsRNA, a significant increase in the TLR3 protein expression was observed in HCDCs, whereas RIG-I protein expression

Table 1 | TLR3/SV40 double immunofluorescence staining in PVAN biopsies

PVAN case no.	Immunofluorescence		TLR3/SV40 colocalization		Interstitial infiltrates
	SV40 positivity	TLR3 positivity	Medullary collecting duct	Cortex	
1	+++ Strong	+ Few, focal	++	++	Moderate
2	+ Few, focal	+ Few	++++	+++	Few
3	(+) Focal	++ Moderate	+++	++++	Few, focal
4	+++ Strong	+ Few	++++	++	Few
5	+ Few	++ Moderate	++	+	Moderate
6	+++ Strong	++ Moderate	++	++	Moderate
7	(+) Focal	+ Few	++++	+	Few, focal
8	(+) Focal	+ Few	+	++	Moderate
9	(+) Focal	++ Moderate	+	+	Moderate
10	+++ Strong	+++ Strong	++++	++++	Absent
11	+ Few	+++ Strong	++	+	Moderate
12	+++ Strong	+++ Strong	+++	++	Severe, diffuse
13	+++ Strong	+ Few	++	++	Moderate
14	+++ Strong	+ Few	+++	+	Few, focal
15	+++ Strong	+ Few	+++	+++	Absent
16	+ Few	+ Few	++++	+++	Few, focal
17	++ Moderate	+++ Strong	++++	++++	Few
18	++ Moderate	+++ Strong	+++	++	Severe, diffuse
19	(+) Focal	++ Moderate	++++	+++	Few, focal

Abbreviations: PVAN, polyomavirus-associated nephropathy; TLR3, Toll-like receptor 3.
TLR3/SV40 colocalization was evaluated semiquantitatively as: +, $<25\%$; ++, $\geqslant 25$ to $<50\%$; +++, $\geqslant 50$ to $<75\%$; ++++, $\geqslant 75\%$.
Highest medullary TLR3/SV40 colocalization rates were found in PVAN biopsies with absent or few and focal interstitial infiltrates. In randomly chosen renal transplant biopsies with negative immunohistochemical SV40 staining, TLR3 expression was nearly absent in proximal tubules, and was strong in dilated atrophic tubules.

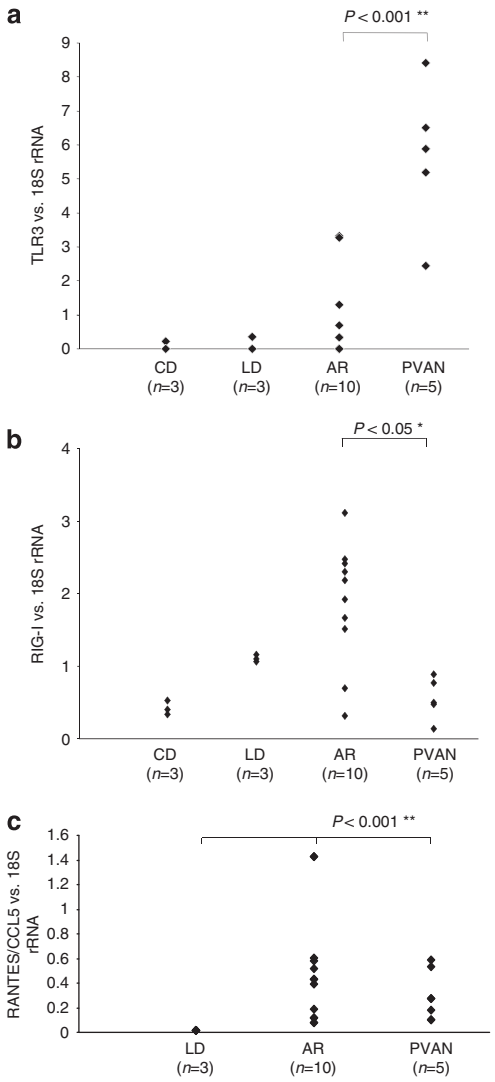

Figure 2 | Toll-like receptor 3 (TLR3), retinoic acid inducible gene-I (RIG-I), and RANTES/CCL5 mRNA expression in the tubulointerstitial compartment of manually microdissected renal transplant biopsies. (**a**) Expression of mRNA for TLR3 shows a significant induction in polyomavirus-associated nephropathy (PVAN) compared with renal allograft biopsies with acute cellular rejection (AR) and pretransplant donor biopsies (cadaveric donor (CD) biopsies and living donor (LD) biopsies). (**b**) In renal allograft biopsies with AR, RIG-I mRNA expression is significantly induced when compared with both controls and biopsies with PVAN. (**c**) RANTES/CCL5 (regulated upon activation, normal T cell expressed and secreted)/(chemokine (C-C motif) ligand 5) was significantly upregulated in AR and PVAN compared with pretransplant donor biopsies from living donors. *$P < 0.05$; **$P < 0.001$.

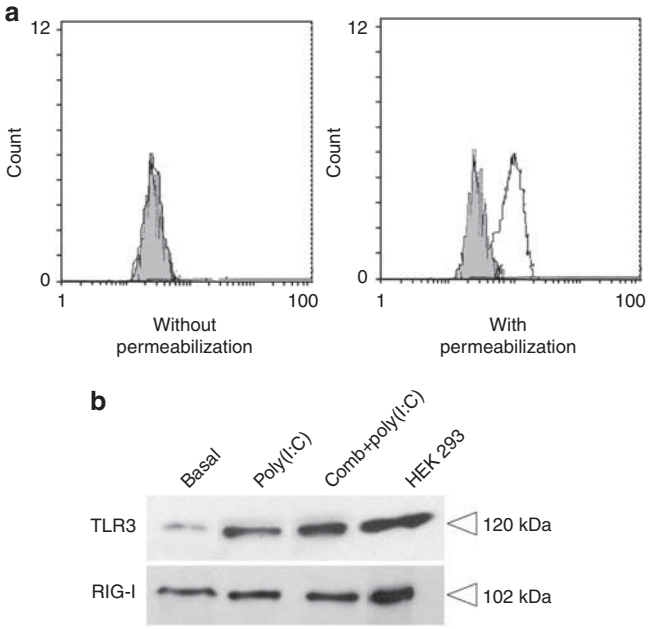

Figure 3 | Localization of Toll-like receptor 3 (TLR3) and expression of TLR3 and retinoic acid inducible gene-1 (RIG-I) in cultured human collecting duct epithelial cells (HCDCs). (**a**) Localization of TLR3 protein by flow cytometry on HCDCs. No TLR3 signal was found on HCDCs without permeabilization, whereas a clear signal for TLR3 was detected after permeabilization. Open histograms represent the fluorescence activity after incubation with a monoclonal anti-TLR3 antibody (Ab). Filled histograms denominate the signal of the appropriate isotype control. Results shown are from one of two independent experiments, which showed reproducible staining patterns. (**b**) Western blot analysis for TLR3 and RIG-I protein expression in HCDCs incubated with 10 μg/ml polyriboinosinic:polyribocytidylic acid (poly(I:C)) with or without prestimulation with a combination of proinflammatory cytokines (tumor necrosis factor-α (TNF-α), interleukin-1β (IL-1β), and interferon-γ (IFN-γ)), or medium alone. HEK 293 cells were used as positive control. Poly(I:C), mimicking viral double-stranded RNA (dsRNA), induced TLR3 and RIG-I protein expression. This effect was potentiated after prestimulation with the combination of cytokines (Comb + poly(I:C)).

showed only a marginal increase. Stimulation with a combination of proinflammatory cytokines (tumor necrosis factor-α (TNF-α), IL-1β, and IFN-γ) and 10 μg/ml poly(I:C) enhanced both TLR3 and RIG-I expression. HEK 293 cells were used as controls and showed a robust TLR3 and RIG-I protein expression.

RNA was prepared from HCDCs growing under standard conditions as well as from HCDCs that had been stimulated with a combination of the cytokines TNF-α, IL-1β, and IFN-γ for different time intervals (0, 6, 12, 24, and 48 h). By real-time RT-PCR, TLR3 mRNA was amplified from both unstimulated (basal) and stimulated (comb) cells. The low basal expression for TLR3 was significantly increased with the cytokine combination in a time-dependent manner up to 48 h (Figure 4a). Similar results were found for RIG-I mRNA expression (Figure 4b).

Incubation with poly(I:C) significantly increased basal TLR3 but not RIG-I mRNA expression (Figure 4c and d) When HCDCs had been pretreated with proinflammatory cytokines, incubation with poly(I:C) (comb + poly(I:C)) markedly enhanced TLR3 and RIG-I mRNA expression. This effect was highly significant compared with basal conditions and with cytokine-stimulated conditions (comb), respectively.

When HCDCs were stimulated with poly(I:C) in increasing concentrations (1, 5, 10, and 100 μg/ml) for 12 h, under

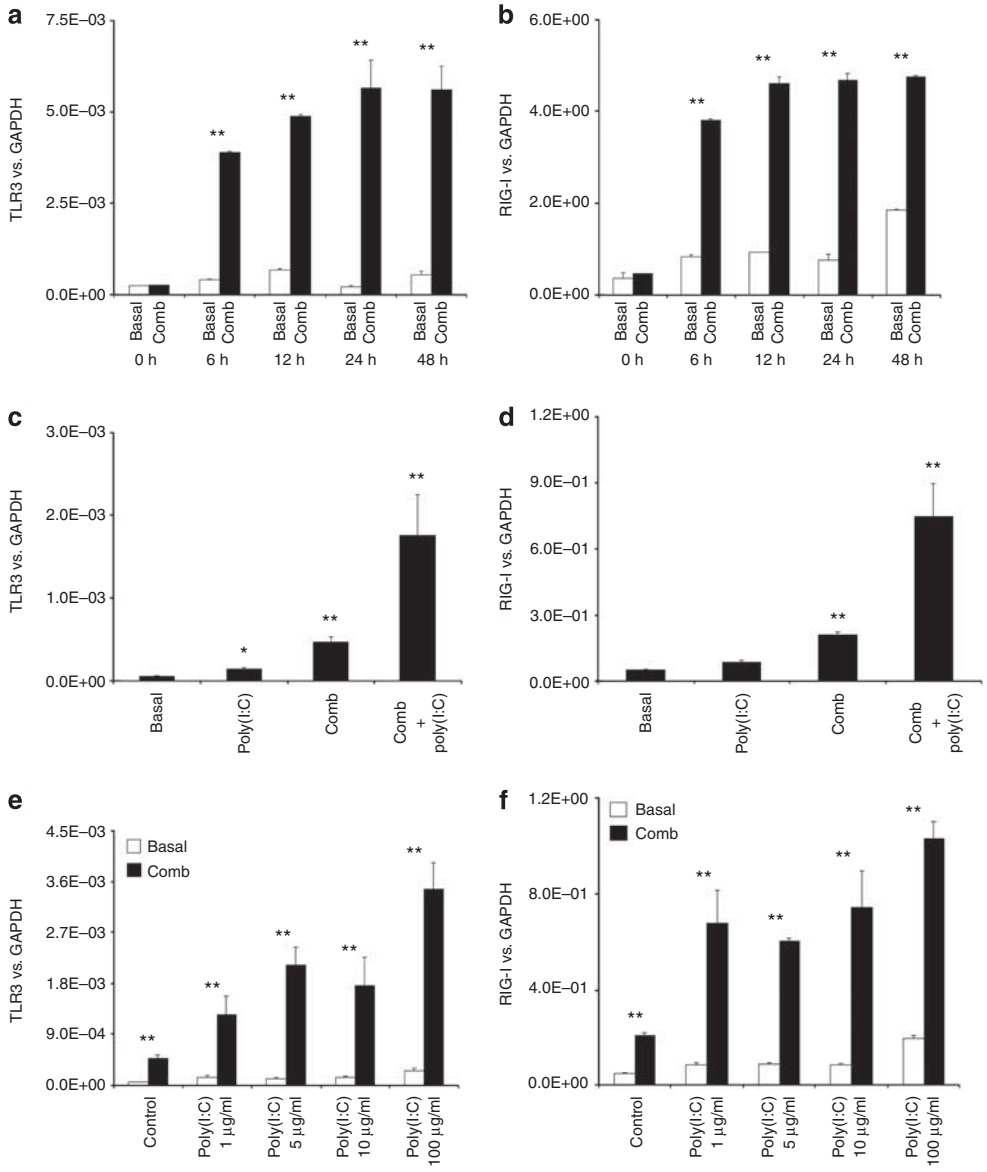

Figure 4 | Expression of Toll-like receptor 3 (TLR3) and retinoic acid inducible gene-I (RIG-I) mRNA on cultured human collecting duct epithelial cells (HCDCs). HCDCs were stimulated with (Comb) or without (Basal) a combination of cytokines (tumor necrosis factor-α (TNF-α), interleukin-1β (IL-1β), and interferon-γ (IFN-γ)) for the times indicated. (**a**) The low basal expression for TLR3 was increased with the cytokine combination in a time-dependent manner up to 48 h. (**b**) Similar results were found for RIG-I mRNA expression. To test the effect of TLR3 and RIG-I activation by polyriboinosinic:polyribocytidylic acid (poly(I:C)), mimicking viral double-stranded RNA (dsRNA), HCDCs were preincubated with (Comb) or without (Basal) the cytokine combination (TNF-α, IL-1β, and IFN-γ) and subsequently stimulated with and without poly(I:C) for 12 h. The mRNA expression for TLR3 and for RIG-I was analyzed by real-time reverse transcriptase-PCR (RT-PCR). HCDCs showed low basal expression for (**c**) TLR3 and (**d**) RIG-I mRNA, which was induced by stimulation with proinflammatory cytokines (Comb). Incubation with poly(I:C) revealed a significant increase of basal TLR3, but not RIG-I, expression. (**e**, **f**) After pretreatment with proinflammatory cytokines, incubation with different concentrations of poly(I:C) (Comb + poly(I:C)) markedly enhanced TLR3 and RIG-I mRNA expression. *$P<0.05$; **$P<0.01$. GAPDH, glyceraldehyde 3-phosphate dehydrogenase.

basal conditions (white columns) only a slight, and not significant, increase for TLR3 and RIG-I was observed. In contrast, when HCDCs were prestimulated with the cytokine combination (black columns), the poly(I:C)-induced TLR3 and RIG-I mRNA expression was significantly increased (Figure 4e and f). Taken together, prestimulation with a combination of proinflammatory cytokines was an essential prerequisite for significant TLR3/RIG-I induction.

Activation of TLR3 and RIG-I by poly(I:C) significantly enhanced the mRNA expression of the proinflammatory cytokine IL-6, the chemokines RANTES/CCL5, MCP-1/CCL2, IL-8/CXCL8, and IP-10/CXCL10, and the antiviral IFN-β

To test the 'downstream' effects of TLR3 activation by poly(I:C) mimicking viral dsRNA in HCDCs, we performed real-time RT-PCR for mRNA expression of selected cytokines and chemokines (IL-6, RANTES/CCL5, MCP-1/CCL2, IL-8/

CXCL8, and IP-10/CXCL10). HCDCs showed low basal expression for IL-6 mRNA. IL-6 expression was significantly induced by stimulation with proinflammatory cytokines (comb). Incubation with poly(I:C) increased IL-6 expression without preconditioning, an effect that was markedly potentiated when HCDCs had been preconditioned with proinflammatory cytokines (comb + poly(I:C)) (Figure 5a) in order to enhance their TLR3 expression. Similar results were obtained for monocyte chemotactic protein-1 (MCP-1)/CCL2 (Figure 5c) and IL-8/CXCL8 (Figure 5d). Expression of RANTES/CCL5 (Figure 5b) could not be increased by poly(I:C) without preconditioning, but was increased by preconditioning with cytokines alone (comb) and even more after cytokine preconditioning followed by additional poly(I:C) stimulation (comb + poly(I:C)). Basal expression for IP-10/CXCL10 (chemokine (C-X-C motif) ligand 10) mRNA (Figure 5e) was not detectable, and after poly(I:C) stimulation, only a slight mRNA expression for IP-10/CXCL10 was found. Pretreatment with the cytokine combination (comb) for 24 h resulted in a significantly increased IP-10/CXCL10 mRNA expression, but remained similar after additional poly(I:C) stimulation (comb + poly(I:C)). For

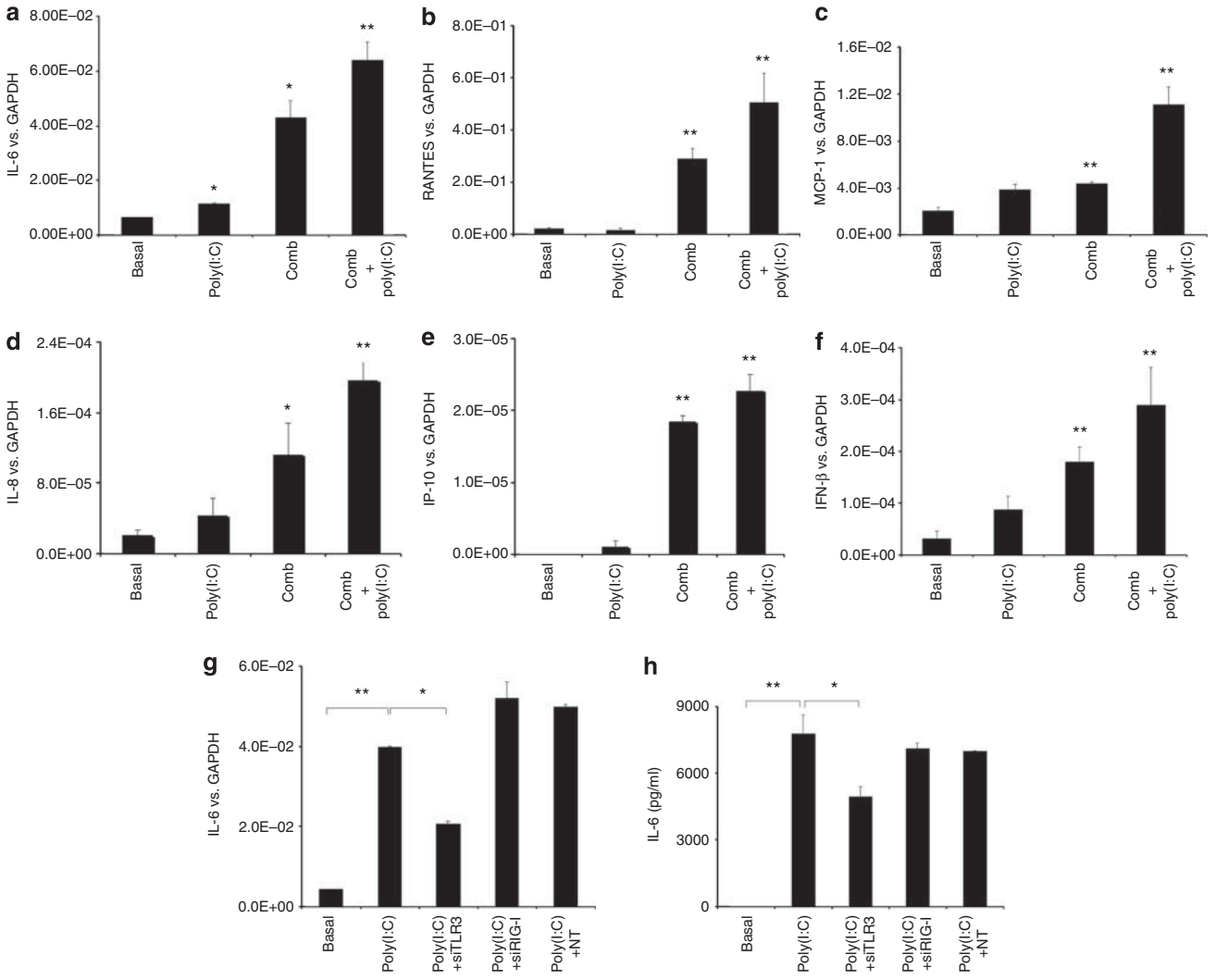

Figure 5 | Effect of polyriboinosinic:polyribocytidylic acid (poly(I:C)) and cytokine prestimulation on the mRNA expression of selected cytokines and chemokines and short interfering RNA (siRNA) experiments for Toll-like receptor 3 (TLR3)/retinoic acid inducible gene-I (RIG-I)-specific knockdown. Human collecting duct epithelial cells (HCDCs) were pretreated with (Comb) or without (Basal) a cytokine combination (tumor necrosis factor-α (TNF-α), interleukin-1β (IL-1β), and interferon-β (IFN-β)) for 24 h and incubated with or without poly(I:C) for 12 h. mRNA levels for (**a**) IL-6, (**c**) MCP-1/CCL2, (**d**) IL-8/CXCL8, and (**e**) IP-10/CXCL10, and (**f**) IFN-β slightly increased after stimulation with poly(I:C). This effect was potentiated after pretreatment with the cytokine combination. (**b**) Expression of RANTES/CCL5 (regulated upon activation, normal T cell expressed and secreted)/(chemokine (C-C motif) ligand 5) was not increased by poly(I:C) without preconditioning, but was increased by preconditioning with cytokines alone (Comb) and even more after cytokine preconditioning followed by additional poly(I:C) stimulation (Comb + poly(I:C)). HCDCs were transfected with siRNA for TLR3 (siTLR3) or RIG-I (siRIG-I) and were stimulated with 10 μg/ml poly(I:C) for 12 h. (**g**) Poly(I:C) significantly increased IL-6 mRNA expression, which was significantly attenuated in cells pretreated with siRNA for TLR3. In contrast, siRNA for RIG-I did not significantly reduce IL-6 mRNA expression. (**h**) Enzyme-linked immunosorbent assay (ELISA) for IL-6 confirmed these results. *$P<0.05$; **$P<0.01$. MCP-1, monocyte chemotactic protein-1; NT, not transfected.

the antiviral IFN-β, basal expression was moderately increased after poly(I:C) stimulation, and, in parallel to the chemokines studied afore, preconditioning with the cytokine combination revealed a significant increase in IFN-β mRNA expression (Figure 5f).

Knockdown of TLR3 with siRNA inhibits the poly(I:C)-induced expression of IL-6 in cultured HCDCs, whereas knockdown of RIG-I had no effect on IL-6 expression

Knockdown experiments using the respective short interfering RNAs (siRNAs) were conducted to evaluate which of the two receptors (TLR3 or RIG-I) might be involved in the IL-6 cytokine response to poly(I:C) stimulation. HCDCs were transfected with siRNA for TLR3 (siTLR3) or RIG-I (siRIG-I) and were stimulated with 10 μg/ml poly(I:C), mimicking viral dsRNA, for 12 h. IL-6 expression was analyzed by *real-time* RT-PCR (Figure 5g) and enzyme-linked immunosorbent assay (ELISA; Figure 5h).

The poly(I:C)-induced IL-6 mRNA expression was significantly attenuated in cells pretreated with siRNA for TLR3. In contrast, siRNA for RIG-I did not significantly reduce the poly(I:C)-induced IL-6 mRNA expression (Figure 5g). ELISA for IL-6 confirmed the poly(I:C)-induced upregulation of IL-6 protein, which was also only attenuated by siRNA for TLR3, but not by siRNA for RIG-I (Figure 5h).

Infection of cultured HCDCs with BKV resulted in a significant increase of cytokine, chemokine, and TLR-3 and RIG-I expression

HCDCs were infected with BKV as described above, to simulate an '*in vivo*' model of BKV infection of the distal nephron segment, and were then incubated for different time intervals (3, 6, 9, 12, and 24 h). As a read-out system for effective viral infection of HCDCs, we analyzed the expression of BKV large T-Ag, representing a marker protein of the early phase of BKV infection. Highest levels of large T-Ag were detected at 3 h post infection by RT-PCR and decreased in a time-dependent manner (Figure 6a). Constitutive expression of BKV large T-Ag was still detectable 48 h after infection, indicating active viral replication (data not shown).

Basal TLR3 and RIG-I mRNA expression showed a slight increase during HCDC culture over 24 h. After infection of HCDCs with BKV, the TLR3 and RIG-I mRNA expression was upregulated markedly at 12 h, and then immediately decreased (Figure 6b and c). The TLR3 adaptor molecule TRIF showed a robust constitutive basal expression in HCDCs, but BKV exposure was not able to enhance TRIF expression in our model, as determined by RT-PCR (data not shown). To test the potential effects of BKV infection on selected cytokine and chemokine generation by HCDCs, we determined IL-6 and IL-8/CXCL8 expression by RT-PCR. Under basal conditions, HCDCs in culture showed a slight constitutive expression of both IL-6 and IL-8.

After BKV exposure, IL-6 mRNA showed a marked increase at 3 h and a moderate, but still highly significant, increase 6 h after infection (Figure 6d). Similar results were obtained for the chemokine IL-8/CXCL8 with a prominent mRNA expression at 3 and 6 h and a return toward baseline at 9 h post infection (Figure 6e). Corresponding protein expression for IL-6 and IL-8/CXCL8 was demonstrated by ELISA. In HCDCs in culture under basal conditions, we found constitutive expression of both IL-6 and IL-8 (Figure 6f and g). After BKV exposure, IL-6 showed a significant and robust increase at all time points, with highest absolute levels at 9 h post infection (Figure 6f). In contrast, the chemokine IL-8/CXCL8 was not elevated at 3 h post infection, but showed a constant significant upregulation at 9, 12, and 24 h after BKV infection (Figure 6g).

Infection of cultured HCDCs with BKV did not lead to activation and upregulation of IL-1β, the NALP-3 inflammasome pathway, and AIM2

Activation of TLR3/RIG-I and robust IL-6, as well as IL-8/CXCL8 upregulation after BKV exposure, was a consistent feature in our '*in vivo*' model of BKV infection. During initial BKV infection of HCDCs, it is likely that different DNA- and RNA-sensing pathways are triggered simultaneously, in order to potentiate antiviral responses to infection. Recognition by these sensing pathways could finally lead to the assembly of inflammasome complexes that activate caspase-1, leading to production of IL-1β and IL-18. To test this hypothesis, we studied the expression of (1) IL-1β, an important pro-inflammatory cytokine that is secreted after assembly of inflammasome complexes, (2) the inflammasome components NALP-3 and caspase-1, and (3) AIM2 (absent in melanoma 2), a newly discovered pathogen recognition receptor involved in the sensing of cytosolic DNA produced by infection with DNA viruses.[31–33] For IL-1β, we found no expression under basal conditions by RT-PCR and ELISA. After BKV infection, we found a slight, but not significant, increase at 6 and 12 h post infection, and a significant increase at 9 h post infection, but this marginal upregulation could not be confirmed by ELISA technique (data not shown). Compatible with this finding, caspase-1 and NALP-3 were absent in our model of BKV infection. AIM2 revealed a slight constitutive expression in HCDCs, which was not increased even after 24 h of BKV infection.

DISCUSSION

Stronger immunosuppressive regimens have decreased the rates of AR in kidney transplantation, but have also led to the emergence of PVAN.[34] Early diagnosis of PVAN by histology in combination with timely reduction in immunosuppression are the only proven measures that can circumvent irreversible parenchymal damage.[35] Despite the critical role that PVAN may have in long-term graft loss, there is surprisingly little known about the immunology of BKV infection. In the current study, we present results suggesting that in PVAN viral dsRNA sensors are involved in the antiviral response.

The presence of viral dsRNA in the cell is a signature of virus infection, which activates cellular sensors of the innate immune system.[11,36] For three reasons we evaluated the

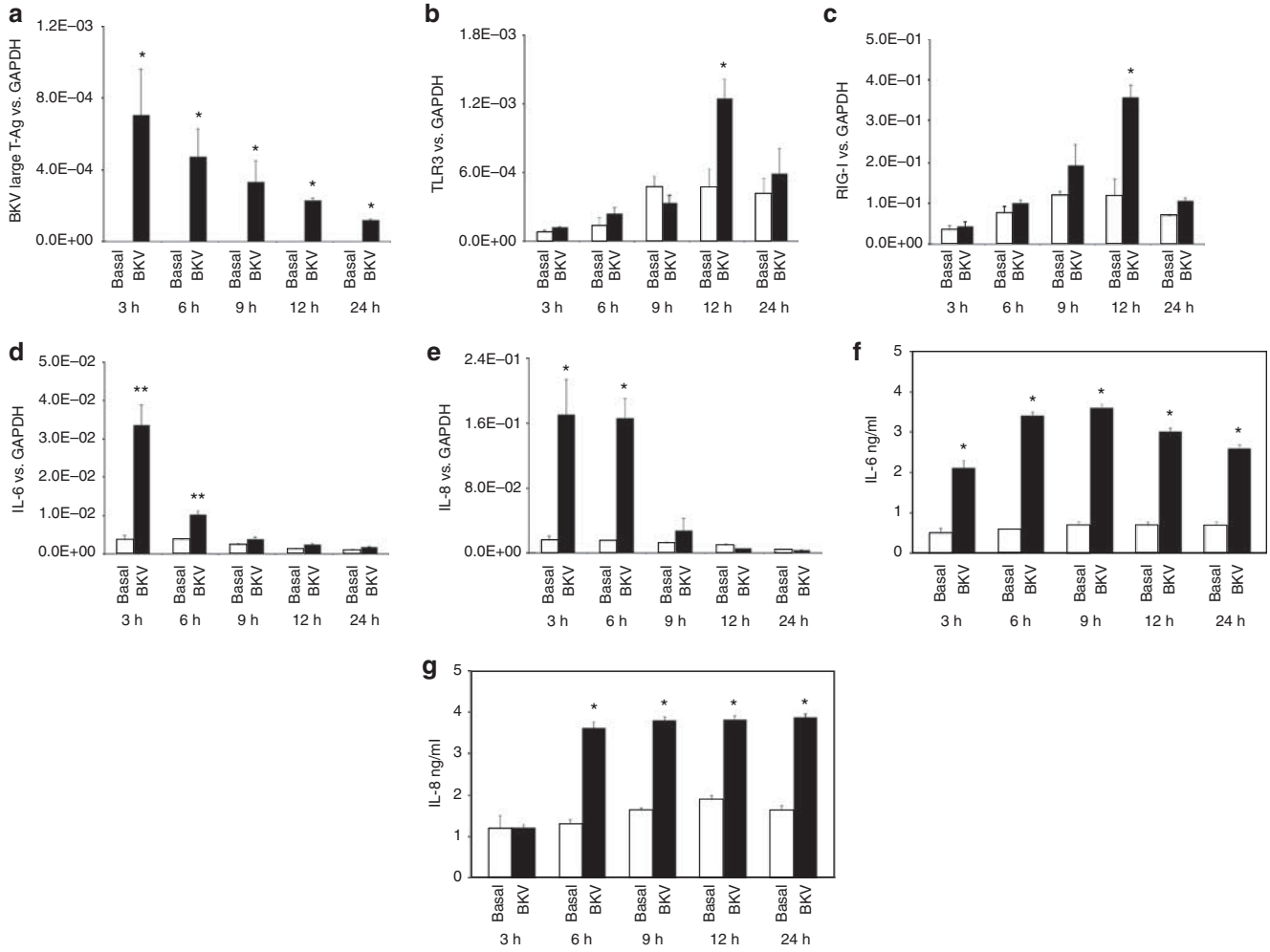

Figure 6 | Infection of cultured human collecting duct epithelial cells (HCDCs) with BK virus (BKV) results in a significant increase of cytokine and chemokine expression and upregulation of double-stranded RNA (dsRNA) receptors Toll-like receptor 3 (TLR3) and retinoic acid inducible gene-I (RIG-I). HCDCs were infected with BKV and were then incubated for different time intervals (3, 6, 9, 12, and 24 h). (**a**) Highest levels of large T antigen (T-Ag), a marker protein of the early phase of BKV infection, were detected at 3 h post infection by reverse transcriptase-PCR (RT-PCR) and decreased in a time-dependent manner. Basal TLR3 and RIG-I mRNA expression showed a slight increase during incubation over 24 h. (**b**, **c**) BKV infection upregulated both receptors at 12 h post infection with a subsequent decrease. (**d**) Under basal conditions, cultured HCDCs showed a low expression of interleukin-6 (IL-6) and IL-8/CXCL8, which increased significantly after BKV exposure. (**e**) Similar results were obtained for the chemokine IL-8/CXCL8. (**f**, **g**) These results were confirmed by enzyme-linked immunosorbent assay (ELISA) technique. $^{*}P<0.05$; $^{**}P<0.01$.

potential role of dsRNA sensors in PVAN. (1) Double-stranded RNA is produced by most viruses (including polyomavirus BK with a circular dsDNA genome) at some point during their replication.[14] (2) During promiscuous transcription, the intracellular concentration of dsRNA is further increased: ~20% of the polyomavirus RNA in infected cells consists of partially ds molecules during transcription in the late stage.[37,38] (3) We recently found BKV RNA in all BKV DNA-positive biopsies, indicating active viral replication, in a gene expression study of renal transplant biopsies.[39]

DsRNA, recognized by specific dsRNA sensors, can lead to the induction of genes associated with inflammation and an antiviral response, including NF-κB target genes, type I IFN, and IFN response genes. TLR3 is not universally required for the generation of effective antiviral responses, and RNA helicases may represent an alternative major cellular sensor for dsRNA.[40] We therefore also looked at RIG-I, which may also function as a cytosolic alternative pattern recognition receptor of viral motifs.[9,15,41] It should be noted that a critical cooperation of the RIG-I/MDA5-type I IFN and the TLR3-type II IFN signaling axes may be required for efficient innate antiviral immune responses.[42]

In human kidney, immunohistochemical staining shows TLR3 expression in glomeruli with a mesangial pattern, in vascular smooth muscle cells of preglomerular vessels, and in collecting duct epithelial cells.[30] Double immunofluorescence staining in PVAN colocalized polyomavirus (anti-SV40) and TLR3 protein expression particularly in epithelial cells of medullary collecting ducts. SV40 large T-Ag showed strong nuclear positivity in the renal epithelium, whereas TLR3 staining was most consistent with tubular intracytoplasmic

and membrane localization. Cellular inflammatory infiltrates and mRNA expression profiles of inflammatory cytokines and chemokines in PVAN and in AR are similar in composition and quantity. This is particularly true for RANTES/CCL5,[43] which was indeed significantly upregulated in both AR and PVAN when compared with controls, thus confirming relevant inflammation. TLR3 mRNA expression segregated PVAN from AR. TLR3, but not RIG-I mRNA expression, was significantly induced in allograft biopsies with PVAN when compared with those with ongoing AR. In contrast, RIG-I mRNA was selectively induced in AR, an observation deserving further investigation.

To further elucidate a potential role of dsRNA receptors in PVAN, we used a cell culture model of collecting tubule origin, the predominant site of renal BK infection.[5] First, we confirmed that the immortalized HCDC line expresses dsRNA receptors under basal conditions. A robust basal mRNA and protein expression for TLR3, as well as for RIG-I, was demonstrated by *real-time* RT-PCR and western blot analysis. TLR3 was localized by FACS analysis in HCDCs intracellularly. Localization of TLR3 in the endosomal membranes of the collecting duct would expose the receptor to the endocytosed virus during BKV infection, as discussed above.

We prestimulated HCDCs with a cytokine combination to establish a proinflammatory milieu in cell culture, as might occur during viral infection. In addition, we exposed the cells to poly(I:C), a synthetic mimetic of viral dsRNA, to simulate aspects of viral infection. The basal expression of both TLR3 and RIG-I mRNA in HCDCs was increased by prestimulation with the combination of cytokines in a dose-dependent manner. The expression of TLR3 and RIG-I mRNA was also enhanced after stimulation with poly(I:C). The concentration of poly(I:C) required for these effects is in the range of those reported by others for these receptors.[44]

Human tubular epithelial cells are known to interact with both neighboring cells and the immune system through the production of cytokines and chemokines such as IL-6, IL-8, IL-15, TNF-α, MCP-1, RANTES, and TGF-β.[45–47] These responses are required to initiate a cellular and humoral immune response to control infection, but can also result in tissue injury and dysfunction, as evidenced in PVAN.[6] Activation of viral receptors by poly(I:C) significantly enhanced the mRNA expression of various cytokines and chemokines (IL-6, IL-8/CXCL8, RANTES/CCL5, MCP-1/CCL2, and IP-10/CXCL10) in HCDCs after poly(I:C) stimulation. These findings are in accordance with data from Mannon *et al.*,[43] who reported elevated levels of RANTES, TNF-α, TNF-β, and activation markers of macrophages in PVAN. In addition, increased urinary excretion of MCP-1 is associated with intragraft tubulointerstitial inflammation in patients with PVAN.[48]

To identify which viral receptors might contribute to the generation of cytokines and chemokines, we knocked down the receptor expression. The poly(I:C)-induced expression of IL-6 was significantly inhibited by transfection with siRNA for TLR3, whereas transfection with siRNA for RIG-I had no significant effect on IL-6, suggesting a pivotal role of TLR3 in this scenario.

Finally, we established an infection model using cultured HCDCs and BKV. After BKV infection, the mRNA expression for IL-6 and IL-8/CXCL8 increased. This early cytokine and chemokine activation was followed by a time-dependent significant increase of TLR3 and RIG-I expression with maxima at 12 h post infection, whereas BKV infection could not further enhance the robust constitutive basal expression of TRIF. Recently, primary human proximal tubule epithelial (HPTE) cells were described as a model for lytic BKV infection.[49] Subsequent studies found a primary activation of genes involved in cell cycle regulation and apoptosis.[50] Of particular note, the HPTE model was not able to elicit an antiviral immune response in the given experimental context.

Our results differ in two major points from the HPTE model: First, in HCDCs, we demonstrated a significant expression of large T-Ag, a marker protein of the early phase of BKV infection, at a very early stage of infection (3 h post infection), whereas in the HPTE model early viral gene expression was first detectable at 24 h post infection with levels increasing out to 72 h. This finding suggests that BKV infection of HCDCs involves particularly the early phase of BKV infection with a more rapid viral trafficking through the cytoplasm than in HPTE cells. Second, the distinctive cytokine and chemokine activation after BKV infection was a prominent early signature in our model. In contrast, a cytokine-targeted PCR array analysis of the HPTE model performed at 4 h post infection revealed no proinflammatory response to BKV infection.[50]

Even basal TLR3 and TRIF expression was sufficient for significant early cytokine/chemokine activation in our infection model. This early activation seems to be independent of efficient virus replication, as demonstrated also in, for example, rhinovirus-induced airway epithelial cells,[51,52] and apparently kick-starts an efficient antiviral response in HCDCs, leading to a transient robust dsRNA receptor expression as demonstrated by significant TLR3 and RIG-I expression.

Activation of TLR3 and RIG-I after stimulation with synthetic dsRNA was a consistent feature in cultured HCDCs, and upregulation of both receptors was confirmed in our infection model mimicking the early infection phase of the collecting duct by BKV. In contrast, we found a robust TLR3, but unexpectedly no significant RIG-I expression in biopsies with PVAN. How can this obvious discrepancy be reconciled? During initial BKV infection of HCDCs, it is likely that different DNA- and RNA-sensing pathways are triggered simultaneously, leading to a parallel upregulation of various receptors. This cross talk between different innate immunity pathways could eventually potentiate antiviral responses to infection. Other potential pathways have been recently suggested,[53,54] but we were not able to demonstrate activation/upregulation of IL-1β, the NALP-3 inflammasome pathway, or AIM2 in our newly established '*in vivo*' model of BKV infection of the distal nephron segment.

A detailed analysis of the observed differences in dsRNA receptor activation between PVAN and AR should now be an important area of future study and could also have a significant impact on the demanding histological differentiation of these two inflammatory conditions. The striking upregulation of RIG-I mRNA expression in AR has now to be confirmed in larger-scale studies and with immunohistochemical or immunofluorescence techniques. On the basis of our findings, it is questionable whether TLR3 mRNA expression analysis or TLR3 immunohistochemistry has the potential to serve as an additional diagnostic tool to discriminate PVAN biopsies from those with acute ongoing rejection, as TLR3 expression is not a unique feature of PVAN. Although TLR3 immunofluorescence signals were most intense in medullary collecting ducts of PVAN, and were independent of concomitant inflammation, we also observed distinct TLR3 staining in cortical atrophic and dilated tubules of AR.

Taken together, we were able to show significant activation of proinflammatory cytokines, chemokines, and the dsRNA receptors TLR3 and RIG-I in cultured HCDCs after poly(I:C) and cytokine stimulation and in a BKV infection model, mimicking polyomavirus BK infection of collecting duct tubules. Immunofluorescence double staining of BKV and TLR3 and mRNA expression analysis of biopsies with PVAN suggest that activation of innate immune defense mechanisms particularly via TLR3 are involved in the antiviral and inflammatory response.

MATERIALS AND METHODS

Preparation of human tissue

For mRNA expression analysis, parts of human renal biopsies were obtained according to the directives of the local ethical committees, and samples were processed according to the protocol of a European multicenter study for gene expression analysis (the European Renal cDNA Bank–Kroener-Fresenius Biopsy Bank (ERCB-KFB)).[55] Microdissected tubulointerstitial specimens from 21 patients were analyzed, including 10 allograft biopsies with acute cellular rejection and 5 allograft biopsies with PVAN. In both groups the Banff histological scores and the immunohistochemical analysis of inflammatory infiltrates were similar. For control biopsies, renal tissue was derived from pretransplantation kidney biopsies during cold ischemia time from three cadaveric (CON CDx, $n=3$) and three living donors (CON LDx, $n=3$).

For double immunofluorescence staining, paraffin-embedded tissue sections from a total of 23 renal allografts, including 19 cases with a histological secured diagnosis of PVAN and 4 randomly chosen transplant biopsies with AR, were obtained from the Department of Cellular and Molecular Pathology at the German Cancer Research Center following guidelines of the respective Ethics Committees.

Immunofluorescence technique for TLR3 and SV40 double staining

For immunofluorescence double staining, 5 µm sections were prepared and mounted on glass slides. After microwave antigen retrieval with citrate buffer, we treated the specimens with blocking buffer and subsequently with primary antibodies against SV40 (1:20; mouse T-Ag; Calbiochem, San Diego, CA) or TLR3 (1:100; anti-human guinea pig), followed by species-specific secondary antibodies as recently described.[56] Specimens were analyzed on a Leica SP5 (Solms, Germany) confocal microscope and confocal stacks were modeled using the Volocity software (Waltham, MA).

Cell culture of immortalized HCDCs

Immortalized HCDCs, provided by H Debiec,[57] were grown in culture medium containing a 1:1 mixture of Dulbecco's modified Eagle's medium and Ham's F12 medium supplemented with 5 µg/ml insulin (Sigma, Taufkirchen, Germany), 5×10^{-8} mol/l dexamethasone (Sigma), 3×10^{-8} mol/l sodium selenite (Sigma), 5 µg/ml transferrine (Sigma), 2 mmol/l glutamine (Gibco, Karlsruhe, Germany), 10 mol/l HEPES Buffer (Gibco), and 2% heat-inactivated fetal bovine serum.

For ELISA and RNA extraction, HCDCs were incubated with a combination of TNF-α (25 ng/ml), IL-1β (10 ng/ml), and IFN-γ (20 ng/ml) for 24 h, washed with phosphate-buffered saline (PBS), incubated in culture medium for 6 h, and washed again with PBS. Subsequently, HCDCs were incubated with medium alone (control) or medium containing poly(I:C) (10 µg/ml) for 12 h. Aliquots of the supernatant medium were removed for ELISA analysis at the time points indicated. For analysis of mRNA levels, extraction of total RNA was performed using an RNeasy Mini Kit (Qiagen, Hilden, Germany) with additional DNase digestion.

Quantitative real-time RT-PCR analysis

Real-time RT-PCR analysis was performed on a TaqMan ABI 7700 sequence detection system (Applied Biosystems, Darmstadt, Germany) using heat-activated *Taq*DNA polymerase (Amplitaq Gold; Applied Biosystems) as described previously.[55] Commercially available predeveloped TaqMan reagents were used for the human target genes (TLR3, gene bank accession number NM_003265/U88879; RIG-I, NM_014314; IL-6, NM_000600; RANTES/CCL5, AF043341; MCP-1/CCL2, X14768; IL-8/CXCL8, Z11686; IP-10/CXCL10, NM_001565; TRIF, Hs01090712_m1; IL-1β, XM010760; caspase-1, Hs00354836_m1; NALP3, Hs00918082_m1; AIM2, Hs00175457_m1) and two endogenous control genes (18S rRNA, 4310893E; GAPDH, M33197; Applied Biosystems). The normalization to both reference (housekeeping) genes yielded comparable results. For detection of BKV large T-Ag sequence, the following primer pair was used: forward: 5′-GGAAAGTCTTTAGGGTCT TCTACCTTT-3′; reverse: 5′-GGTGCCAACCTATGGAACAGA-3′; specific probe: 5′-AATCTGCTGTTGCTTCTTCATCACTGGCA-3′, FAM and TAMRA labeled.[31] All measurements were recorded in duplicates. Controls consisting of bidistilled H_2O were negative in all runs.

FACS analysis for TLR3

For FACS analysis, cultured HCDCs were detached with PBS/10 mmol/l EDTA (pH 8) and stained for TLR3 using a specific mouse monoclonal antibody (eBioscience, San Diego, CA) and a fluorescein isothiocyanate rabbit secondary antibody against mouse $F(ab)_2$ fragment (F0232; Dako, Glostrup, Denmark) as described.[30] For intracellular staining, HCDCs were treated with Cytofix/Cytoperm Reagent (BD Biosciences, San Jose, CA) followed by monoclonal antibody against TLR3 and secondary antibody incubations in saponin buffer. The TLR3 signal was analyzed using a FACSCalibur with CellQuest analysis software (Becton-Dickinson, Heidelberg, Germany). Appropriate IgG isotype preparations

(mouse IgG1 clone MOPC 21, Sigma) were used to control for unspecific staining.

Western immunoblot analysis for TLR3 and RIG-I

After incubation with poly(I:C) with or without prestimulation with proinflammatory cytokines, HCDCs were lysed with radioimmunoprecipitation assay buffer (50 mmol/l Tris-HCL, pH 8; 150 mmol/l NaCl; 1% NP-40; 0.5% sodium deoxycholate; 0.1% SDS) containing protease inhibitors. The lysates were cleared by centrifugation at 13,000 *g* for 15 min at 4 °C and protein concentration was determined with the DC protein assay kit (Bio-Rad Laboratories, Munich, Germany). Proteins (40 μg/ml) were separated by sodium dodecyl sulfate-polyacrylamide on an 8% polyacrylamide gel and transferred to a polyvinylidene fluoride membrane for western blotting (Immobilon-P Transfer Membrane; Millipore, Schwalbach, Germany). The membranes were blocked in 3% milk solution in Tris-buffered saline/Tween 20 (TLR3) or 5% bovine serum albumin (RIG-I) for 1 h and probed overnight with a monoclonal antibody against human TLR3 (Acris Antibodies, Hiddenhausen, Germany) or human RIG-I provided by Dr Simon Rothenfusser.[58]

After washing four times in Tris-buffered saline with Tween-20, the membranes were incubated with secondary purified rabbit anti-mouse IgG (H&L)-HRP (TLR3) or secondary peroxidase-conjugated AffiniPure Goat Anti-Rat IgG + IgM (H + L) (RIG-I) for 1 h and washed again four times with Tris-buffered saline with Tween-20. Signals were visualized with a Western Lightning Chemiluminescence reagent plus Kit (Perkin Elmer, Waltham, MA).

ELISA

ELISAs for IL-6, IL-8, and IL-1β were performed on cell culture supernatants using commercial assay kits (Quantikine, R&D Systems, Minneapolis, MN) following the provider's instructions.

Knockdown of gene expression with siRNA

Predesigned siRNA for TLR3 and RIG-I was purchased from Ambion (Tokyo, Japan). Transfection of siRNA into the cells was performed over 24 h as described.[59] Scrambled siRNA was used as the nonspecific negative control of siRNA (Ambion).

Polyomavirus BK preparation and infection of HCDCs with polyomavirus (type BK) derived from patients with BKV reactivation

For BK virus isolation, a urine sample with a viral load of $>10^8$ copies/ml from a patient with a known BKV reactivation was used. The sample was inoculated for 1 h on Vero cells before minimal essential medium/2% fetal calf serum was added. Viral propagation was monitored in the supernatant by quantitative real-time PCR with an in-house test on a 7500 Fast Real-Time PCR System (Applied Biosystems, Darmstadt, Germany) using primers from the large T-Ag region and a VIC-labeled probe (see above). At a load of 10^9 copies/ml, virus was harvested by centrifugation of the supernatant and subsequently passaged on HEK 293 cells with minimal essential medium/2% fetal calf serum for 60 days. Infected cells were split at 10-day intervals. Viral growth was monitored by quantitative PCR and by immunofluorescence against T-Ag (Abcam, Cambridge, MA). To isolate BKV, HEK 293 cells were lysed by repeated freeze–thaw cycles (three times) and subsequent centrifugation at 800 *g* for 30 min. The supernatant was adjusted to 5000 focus-forming units per ml with PBS and stored at −80 °C. For experiments, virus was dissolved in culture medium and HCDCs were stimulated as indicated (1 ml medium per well).

Statistical analysis

Values are provided as mean ± s.e.m. Statistical analysis was performed by unpaired *t*-test if applicable or by analysis of variance. Significant differences are indicated for *P*-values <0.05 (*) or 0.01 (**), respectively.

DISCLOSURE

All the authors declared no competing interests.

ACKNOWLEDGMENTS

The expert technical support of Claudia Schmidt is gratefully acknowledged. This study was supported in part by the National Institutes of Health (National Institute of Diabetes and Digestive and Kidney Diseases R01-DK081420-01 to DS), the SFB405 B10 (to HJG), the Else Kröner-Fresenius Foundation (to MW and CDC), the Peter-Stiftung, the Fritz Bender Stiftung, and the Deutsche Vereinigung zur Bekämpfung von Viruskrankheiten (to MW). We thank all participating centers of the European Renal cDNA Bank–Kröner-Fresenius Biopsy Bank and their patients for their cooperation. Active members at the time of the study were Clemens David Cohen, Holger Schmid, Michael Fischereder, Lutz Weber, Matthias Kretzler, and Detlef Schlöndorff, Munich/Zurich/Ann Arbor/New York; Jean Daniel Sraer and Pierre Ronco, Paris; Maria Pia Rastaldi and Giuseppe D'Amico, Milan; Peter Doran and Hugh Brady, Dublin; Detlev Mönks and Christoph Wanner, Würzburg; Andrew Rees, Aberdeen; Frank Strutz and Gerhard Anton Müller, Göttingen; Peter Mertens and Jürgen Floege, Aachen; Norbert Braun and Teut Risler, Tübingen; Loreto Gesualdo and Francesco Paolo Schena, Bari; Jens Gerth and Gunter Wolf, Jena; Rainer Oberbauer and Dontscho Kerjaschki, Vienna; Bernhard Banas and Bernhard Krämer, Regensburg; Moin Saleem, Bristol; Rudolf Wüthrich, Zurich; Walter Samtleben, Munich; Harm Peters and Hans-Hellmut Neumayer, Berlin; Mohamed Daha, Leiden; Katrin Ivens and Bernd Grabensee, Düsseldorf; Francisco Mampaso (deceased), Madrid; Jun Oh, Franz Schaefer, Martin Zeier, and Hermann-Joseph Gröne, Heidelberg; Peter Gross, Dresden; Giancarlo Tonolo, Sassari; Vladimir Tesar, Prague; Harald Rupprecht, Bayreuth; and Hans-Peter Marti, Bern.

SUPPLEMENTARY MATERIAL

Table S1. Histological findings and diagnoses in renal transplant biopsies included in the mRNA expression analysis.
Supplementary material is linked to the online version of the paper at http://www.nature.com/ki

REFERENCES

1. Hirsch HH. Polyomavirus BK nephropathy: a (re-)emerging complication in renal transplantation. *Am J Transplant* 2002; **2**: 25–30.
2. Nickeleit V, Singh HK, Mihatsch MJ. Polyomavirus nephropathy: morphology, pathophysiology, and clinical management. *Curr Opin Nephrol Hypertens* 2003; **12**: 599–605.
3. Funk GA, Gosert R, Comoli P *et al.* Polyomavirus BK replication dynamics in vivo and in silico to predict cytopathology and viral clearance in kidney transplants. *Am J Transplant* 2008; **8**: 2368–2377.
4. Jiang M, Abend JR, Tsai B *et al.* Early events during BK virus entry and disassembly. *J Virol* 2009; **83**: 1350–1358.
5. Meehan SM, Kraus MD, Kadambi PV *et al.* Nephron segment localization of polyoma virus large T antigen in renal allografts. *Hum Pathol* 2006; **37**: 1400–1406.
6. Liptak P, Kemeny E, Ivanyi B. Primer: histopathology of polyomavirus-associated nephropathy in renal allografts. *Nat Clin Pract Nephrol* 2006; **2**: 631–636.
7. Moriyama T, Marquez JP, Wakatsuki T *et al.* Caveolar endocytosis is critical for BK virus infection of human renal proximal tubular epithelial cells. *J Virol* 2007; **81**: 8552–8562.
8. Comoli P, Binggeli S, Ginevri F *et al.* Polyomavirus-associated nephropathy: update on BK virus-specific immunity. *Transpl Infect Dis* 2006; **8**: 86–94.
9. Takeuchi O, Akira S. Innate immunity to virus infection. *Immunol Rev* 2009; **227**: 75–86.

10. Akira S, Uematsu S, Takeuchi O. Pathogen recognition and innate immunity. *Cell* 2006; **124**: 783–801.
11. Meylan E, Tschopp J. Toll-like receptors and RNA helicases: two parallel ways to trigger antiviral responses. *Mol Cell* 2006; **22**: 561–569.
12. Alnemri ES. Sensing cytoplasmic danger signals by the inflammasome. *J Clin Immunol* 2010; **30**: 512–519.
13. Schroder K, Tschopp J. The inflammasomes. *Cell* 2010; **140**: 821–832.
14. Alexopoulou L, Holt AC, Medzhitov R *et al.* Recognition of double-stranded RNA and activation of NF-kappaB by Toll-like receptor 3. *Nature* 2001; **413**: 732–738.
15. Pichlmair A, Schulz O, Tan CP *et al.* RIG-I-mediated antiviral responses to single-stranded RNA bearing 5′-phosphates. *Science* 2006; **314**: 997–1001.
16. Anders HJ, Lichtnekert J, Allam R. Interferon-alpha and -beta in kidney inflammation. *Kidney Int* 2010; **77**: 848–854.
17. Kato H, Sato S, Yoneyama M *et al.* Cell type-specific involvement of RIG-I in antiviral response. *Immunity* 2005; **23**: 19–28.
18. Yoneyama M, Kikuchi M, Matsumoto K *et al.* Shared and unique functions of the DExD/H-box helicases RIG-I, MDA5, and LGP2 in antiviral innate immunity. *J Immunol* 2005; **175**: 2851–2858.
19. Hornung V, Ellegast J, Kim S *et al.* 5′-Triphosphate RNA is the ligand for RIG-I. *Science* 2006; **314**: 994–997.
20. Chiu YH, Macmillan JB, Chen ZJ. RNA polymerase III detects cytosolic DNA and induces type I interferons through the RIG-I pathway. *Cell* 2009; **138**: 576–591.
21. Benigni A, Caroli C, Longaretti L *et al.* Involvement of renal tubular Toll-like receptor 9 in the development of tubulointerstitial injury in systemic lupus. *Arthritis Rheum* 2007; **56**: 1569–1578.
22. Matsumoto M, Kikkawa S, Kohase M *et al.* Establishment of a monoclonal antibody against human Toll-like receptor 3 that blocks double-stranded RNA-mediated signaling. *Biochem Biophys Res Commun* 2002; **293**: 1364–1369.
23. Matsumoto M, Funami K, Oshiumi H *et al.* Toll-like receptor 3: a link between toll-like receptor, interferon and viruses. *Microbiol Immunol* 2004; **48**: 147–154.
24. Yamamoto M, Sato S, Hemmi H *et al.* Role of adaptor TRIF in the MyD88-independent Toll-like receptor signaling pathway. *Science* 2003; **301**: 640–643.
25. Johnsen IB, Nguyen TT, Ringdal M *et al.* Toll-like receptor 3 associates with c-Src tyrosine kinase on endosomes to initiate antiviral signaling. *EMBO J* 2006; **25**: 3335–3346.
26. West J, Damania B. Upregulation of the TLR3 pathway by Kaposi's sarcoma-associated herpesvirus during primary infection. *J Virol* 2008; **82**: 5440–5449.
27. Zhang SY, Jouanguy E, Ugolini S *et al.* TLR3 deficiency in patients with herpes simplex encephalitis. *Science* 2007; **317**: 1522–1527.
28. Préhaud C, Mégret F, Lafage M *et al.* Virus infection switches TLR-3-positive human neurons to become strong producers of beta interferon. *J Virol* 2005; **79**: 12893–12904.
29. Tabeta K, Georgel P, Janssen E *et al.* Toll-like receptors 9 and 3 as essential components of innate immune defense against mouse cytomegalovirus infection. *Proc Natl Acad Sci USA* 2004; **101**: 3516–3521.
30. Wörnle M, Schmid H, Banas B *et al.* Novel role of toll-like receptor 3 in hepatitis C-associated glomerulonephritis. *Am J Pathol* 2006; **168**: 370–385.
31. Thornberry NA, Bull HG, Calaycay JR *et al.* A novel heterodimeric cysteine protease is required for interleukin-1 beta processing in monocytes. *Nature* 1992; **356**: 768–774.
32. Pétrilli V, Dostert C, Muruve DA *et al.* The inflammasome: a danger sensing complex triggering innate immunity. *Curr Opin Immunol* 2007; **19**: 615–622.
33. Fernandes-Alnemri T, Yu JW, Datta P *et al.* AIM2 activates the inflammasome and cell death in response to cytoplasmic DNA. *Nature* 2009; **458**: 509–513.
34. Ramos E, Drachenberg CB, Wali R *et al.* The decade of polyomavirus BK-associated nephropathy: state of affairs. *Transplantation* 2009; **87**: 621–630.
35. Johnston O, Jaswal D, Gill JS *et al.* Treatment of polyomavirus infection in kidney transplant recipients: a systematic review. *Transplantation* 2010; **89**: 1057–1070.
36. Kawai T, Akira S. Innate immune recognition of viral infection. *Nat Immunol* 2006; **7**: 131–137.
37. Fried AH. Density heterogeneity of simian virus 40 ribonucleic acid late after infection of permissive cells. *J Virol* 1972; **10**: 1236–1239.
38. Aloni Y. Extensive symmetrical transcription of Simian Virus 40 DNA in virus-yielding cells. *Proc Natl Acad Sci USA* 1972; **69**: 2404–2409.
39. Schmid H, Nitschko H, Gerth J *et al.* Polyomavirus DNA and RNA detection in renal allograft biopsies: results from a European multicenter study. *Transplantation* 2005; **80**: 600–604.
40. Kawai T, Akira S. Toll-like receptor and RIG-I-like receptor signaling. *Ann NY Acad Sci* 2008; **1143**: 1–20.
41. Yoneyama M, Fujita T. RNA recognition and signal transduction by RIG-I-like receptors. *Immunol Rev* 2009; **227**: 54–65.
42. Negishi H, Osawa T, Ogami K *et al.* A critical link between Toll-like receptor 3 and type II interferon signaling pathways in antiviral innate immunity. *Proc Natl Acad Sci USA* 2008; **105**: 20446–20451.
43. Mannon RB, Hoffmann SC, Kampen RL *et al.* Molecular evaluation of BK polyomavirus nephropathy. *Am J Transplant* 2005; **5**: 2883–2893.
44. Kato H, Takeuchi O, Mikamo-Satoh E *et al.* Length-dependent recognition of double-stranded ribonucleic acids by retinoic acid-inducible gene-I and melanoma differentiation-associated gene 5. *J Exp Med* 2008; **205**: 1601–1610.
45. Schmouder RL, Strieter RM, Wiggins RC *et al.* In vitro and in vivo interleukin-8 production in human renal cortical epithelia. *Kidney Int* 1992; **41**: 191–198.
46. Schmouder RL, Strieter RM, Kunkel SL. Interferon-gamma regulation of human renal cortical epithelial cell-derived monocyte chemotactic peptide-1. *Kidney Int* 1993; **44**: 43–49.
47. Daha MR, van Kooten C. Is the proximal tubular cell a proinflammatory cell? *Nephrol Dial Transplant* 2000; **15**(Suppl 6): 41–43.
48. Rybka K *et al.* Immunocytological urinalysis and monocyte chemotactic peptide-1 in renal transplant recipients with polyomavirus replication. *Transplant Proc* 2006; **38**: 151–154.
49. Low J, Humes HD, Szczypka M *et al.* BKV and SV40 infection of human kidney tubular epithelial cells in vitro. *Virology* 2004; **323**: 182–188.
50. Abend JR, Low JA, Imperiale MJ. Global effects of BKV infection on gene expression in human primary kidney epithelial cells. *Virology* 2010; **397**: 73–79.
51. Newcomb DC, Sajjan U, Nanua S *et al.* Phosphatidylinositol 3-kinase is required for rhinovirus-induced airway epithelial cell interleukin-8 expression. *J Biol Chem* 2005; **280**: 36952–36961.
52. Griego SD, Weston CB, Adams JL *et al.* Role of p38 mitogen-activated protein kinase in rhinovirus-induced cytokine production by bronchial epithelial cells. *J Immunol* 2000; **165**: 5211–5220.
53. Ablasser A, Bauernfeind F, Hartmann G *et al.* RIG-I-dependent sensing of poly(dA:dT) through the induction of an RNA polymerase III-transcribed RNA intermediate. *Nat Immunol* 2009; **10**: 1065–1072.
54. Bürckstümmer T, Baumann C, Blüml S *et al.* An orthogonal proteomic-genomic screen identifies AIM2 as a cytoplasmic DNA sensor for the inflammasome. *Nat Immunol* 2009; **10**: 266–272.
55. Cohen CD, Frach K, Schlöndorff D *et al.* Quantitative gene expression analysis in renal biopsies: a novel protocol for a high-throughput multicenter application. *Kidney Int* 2002; **61**: 133–140.
56. Kessenbrock K, Krumbholz M, Schönermarck U *et al.* Netting neutrophils in autoimmune small-vessel vasculitis. *Nat Med* 2009; **15**: 623–625.
57. Prié D, Friedlander G, Coureau C *et al.* Role of adenosine on glucagon-induced cAMP in a human cortical collecting duct cell line. *Kidney Int* 1995; **47**: 1310–1318.
58. Schmidt A, Schwerd T, Hamm W *et al.* 5′-triphosphate RNA requires base-paired structures to activate antiviral signaling via RIG-I. *Proc Natl Acad Sci USA* 2009; **106**: 12067–12072.
59. Matsukura S, Kokubu F, Kurokawa M *et al.* Role of RIG-I, MDA-5, and PKR on the expression of inflammatory chemokines induced by synthetic dsRNA in airway epithelial cells. *Int Arch of Allergy Immunol* 2007; **143**: 80–83.